

Accelerating the Convergence and Reducing the Variance of Path Integral Calculations of Quantum Mechanical Free Energies by Using Local Reference Potentials

Steven L. Mielke* and Donald G. Truhlar*

Department of Chemistry and Supercomputing Institute, University of Minnesota, 207 Pleasant St. S.E., Minneapolis, Minnesota 55455-0431, United States

S Supporting Information

ABSTRACT: We present two new methods to accelerate the convergence of Feynman path integral calculations of thermodynamic partition functions. The first enhancement uses information from instantaneous normal mode (INM) calculations to decrease the number of discretized points necessary to represent the Feynman paths and is denoted the local generalized Pitzer–Gwinn (LGPG) scheme. The second enhancement, denoted harmonically guided variance reduction (HGVR), reduces the variance in Monte Carlo (MC) calculations by exploiting the correlation between the sampling error associated with the sum over paths at a particular centroid location for the accurate potential and for the INM approximation of a model potential, the latter of which can be exactly calculated. The LGPG scheme can reduce the number of quadrature points required along the paths by nearly an order of magnitude, and the HGVR scheme can reduce the number of MC samples needed to achieve a target accuracy by more than an order of magnitude. Numerical calculations are presented for H_2O_2 , a very anharmonic system where torsional motion is important, and H_2O , a system more amenable to harmonic reference treatment.

1. INTRODUCTION

Feynman path integrals,^{1,2} together with Monte Carlo (MC) integration,³ provide a convenient framework for the evaluation of accurate quantum mechanical (QM) partition functions in a formalism that takes advantage of many of the economies available in the classical limit of quantum mechanics. However, a QM treatment, especially at low temperatures, can involve considerably greater computational effort than a classical mechanical treatment. Consequently, much research has been directed to methods for improving the computational efficiency^{4–30} of path integral calculations or to making useful approximations.^{31–40}

We use mass-scaled coordinates \mathbf{q} , where all coordinates are scaled to a common reduced mass μ . In the classical limit (CL), the partition function for an NVT ensemble is a phase space integral:

$$Q^{\text{CL}} = \frac{1}{(2\pi\hbar)^N \sigma_{\text{sym}}} \int d\mathbf{q} d\mathbf{p} \exp[-\beta H(\mathbf{q}, \mathbf{p})] \quad (1)$$

where σ_{sym} is an identical-atom permutational symmetry number, H is the Hamiltonian, β is $1/(k_{\text{B}}T)$, k_{B} is Boltzmann's constant, T is temperature, N is the dimensionality of the coordinate space, and the set of momenta conjugate to \mathbf{q} is denoted \mathbf{p} . Then integration over the momentum space leads to a configurational integral:

$$Q^{\text{CL}} = \frac{1}{\sigma_{\text{sym}}} \left(\frac{\mu}{2\pi\hbar^2\beta} \right)^{N/2} \int d\mathbf{q} \exp[-\beta V(\mathbf{q})] \quad (2)$$

where $V(\mathbf{q})$ is the potential energy. In comparison, the QM partition function may be evaluated via Feynman path integrals as

$$Q^{\text{QM}} = \frac{1}{\sigma_{\text{sym}}} \int d\mathbf{q}_c \oint D\mathbf{q}(s) \delta(\mathbf{q}_c - \bar{\mathbf{q}}) \times \exp \left[\frac{-1}{\hbar} \int_0^{\hbar\beta} ds \left(\frac{\mu}{2} \left\{ \frac{d\mathbf{q}(s)}{ds} \right\}^2 + V[\mathbf{q}(s)] \right) \right] \quad (3)$$

where s is imaginary time, $\oint D\mathbf{q}(S)$ denotes a sum over all closed paths $\mathbf{q}(S)$, and $\bar{\mathbf{q}}$ is the path centroid given by

$$\bar{\mathbf{q}} = \frac{1}{\hbar\beta} \int_0^{\hbar\beta} ds \mathbf{q}(s) \quad (4)$$

In writing eq 3 we have chosen to reorganize the integral $\oint D\mathbf{q}(S)$ into a double integral where we first consider only paths having a particular centroid location, \mathbf{q}_c , and then integrate over all possible centroid locations. Sorting the paths by their centroid location, which is a practice originally introduced by Feynman and Hibbs,¹ will be important for the development of the new methods presented below and is also convenient for importance sampling purposes.

The additional work involved in evaluating eq 3 compared to eq 2 comes from two distinct sources. For each point, \mathbf{q}_c in configuration space, the QM calculation requires a sum over all possible paths having that point as its centroid, whereas the classical limit calculation involves only a single value of the potential energy at that point. In the context of an MC calculation, this will lead to an increased sampling variance, and hence, the need for a larger number of samples for a given level of accuracy. The second source of additional work comes from the need to perform the integration over the paths, which can

Received: February 4, 2012

Published: April 5, 2012



require many evaluations of the potential to achieved converged results. In the present article we present two methods employing instantaneous normal mode (INM) reference potentials: one method accelerates the convergence of the integration of Feynman paths, and the second reduces the variance associated with the need to sum over all possible paths.

2. THEORY

2.1. Numerical Treatment of Feynman Path Integrals.

Equation 3 is not in a convenient form for numerical evaluation. First we remove the motion of the center of mass so that the coordinate space has dimension N equal to $3n^A - 3$, where n^A is the number of atoms in the molecular system under consideration. This means we are calculating the barycentric partition function, not the full one, which also has overall translation. Because the system we are considering is bound, we can then reduce the hypervolume of the space to be included in the integrations to a finite domain Γ . We choose to perform the integration over the paths using a $(P + 1)$ -point trapezoidal-rule quadrature with the quadrature nodes denoted $\mathbf{q}_1, \mathbf{q}_2, \dots, \mathbf{q}_{P+1}$, where $\mathbf{q}_{P+1} \equiv \mathbf{q}_1$; partition functions obtained with this integration will be denote $Q^{[P]}$. We begin with the discretized path integral approximation given by

$$Q^{[P]} = \frac{Q_{\text{fp}}(T)}{\sigma_{\text{sym}}} \times \frac{\int_{\Gamma} d\mathbf{q}_c \oint D[\mathbf{q}(s)] \delta(\mathbf{q}_c - \bar{\mathbf{q}}) \Phi^{\text{fp}}[\mathbf{q}(s)] \exp\left\{-\frac{\beta}{P} \sum_{i=1}^P V(\mathbf{q}_i)\right\}}{\int_{\Gamma} d\mathbf{q}_c \oint D[\mathbf{q}(s)] \delta(\mathbf{q}_c - \bar{\mathbf{q}}) \Phi^{\text{fp}}[\mathbf{q}(s)]} \quad (5)$$

where the superscript on the left-hand side denotes that it is a finite- P approximation, and we denote the contribution of a particular path for a free-particle (i.e., where the potential is zero) as $\Phi^{\text{fp}}[\mathbf{q}(S)]$ where

$$\Phi^{\text{fp}} = \exp\left[-\frac{1}{\hbar} \int_0^{\hbar\beta} ds \frac{\mu}{2} \left\{ \frac{d\mathbf{q}(s)}{ds} \right\}^2\right] \quad (6)$$

The derivation of eq 5 is presented elsewhere;¹² note that the formula becomes exact as P tends to infinity. The use of trapezoidal-rule quadrature in eq 5 is referred to¹² as the trapezoidal Trotter (TT) approximation or the discretized path integral approximation.

Note that the denominator of eq 5 is the free particle partition function given by

$$Q_{\text{fp}} = V_{\Gamma} \left(\frac{\mu}{2\pi\hbar^2\beta} \right)^{N/2} \quad (7)$$

but writing the result in the long form, as in eq 5, shows that the procedure corresponds to calculating an average of $\exp\{-(\beta/P) \sum_{i=1}^P V(\mathbf{q}_i)\}$ for samples where the path centroid \mathbf{q}_c is taken from a uniform distribution within Γ , and where the paths are selected from a free-particle distribution.

As a practical matter, instead of uniformly sampling \mathbf{q}_c we employ stratified sampling using the potential energy at the centroid position, and we also employ importance sampling using methods presented previously;^{8,12,41} the details of these methods do not influence the implementation of the new methods to be presented below, so these details are presented in the Appendix Section to avoid distraction while we explain the new ideas.

Partition functions calculated in the TT approximation of eq 5 converge as $O(1/P)^2$.⁴² However, we may readily extrapolate to the $P \rightarrow \infty$ limit using the enhanced same path (ESP) scheme.¹⁰ Let P^{max} be the largest P to be explicitly calculated. For values of P that are divisors of P^{max} , the ESP scheme employs estimators that converge monotonically with respect to P on a path-by-path basis; because the information needed for calculations with these P is already available from the calculations with $P = P^{\text{max}}$, the extrapolation ($P \rightarrow \infty$) is essentially free of cost. The ESP extrapolated results are labeled $Q^{[P=\infty]}$, and they are obtained by fitting results for several values of P to the functional form:

$$Q^{[P]} = Q^{[P=\infty]} + \frac{C_1}{P^2} + \frac{C_2}{P^3} \quad (8)$$

where $Q^{[P=\infty]}$, C_1 , and C_2 are fitting parameters; the extrapolated results converge as $(1/P)^4$. Most other approaches^{26,27,43–45} that converge faster than quadratically in $1/P$ require information about derivatives of the potential. A variant¹⁷ of the method of Predescu and co-workers^{13–15,17} also achieves $O[(1/P)^4]$ convergence while requiring only potential evaluations; however, the two new methods presented below make use of analytical expressions for finite- P results that are not now available for this scheme.

As mentioned above, we only consider the internal degrees of freedom in the present discussion; if desired, contributions from translational motion may be added using ideal gas expressions. The barycentric free energy may be calculated from

$$G = A = -RT \ln Q \quad (9)$$

where Q is approximated by $Q^{[P=\infty]}$. All partition functions in the present article have the zero of energy chosen as the global minimum potential energy.

2.2. Pitzer–Gwinn Schemes. Attempts to add quantum effects to classical phase space integrals preceded the development of Feynman path integrals. In 1942 Pitzer and Gwinn⁴⁶ (PG) recommended a scheme for adding quantum effects to an accurate classical calculation using harmonic partition functions calculated using the equilibrium geometry via

$$Q^{\text{PG}} = \left(\frac{Q^{\text{QHO}}}{Q^{\text{CHO}}} \right) Q^{\text{classical}} \quad (10)$$

where Q^{QHO} and Q^{CHO} denote the partition function for a quantal and classical harmonic oscillator (HO), respectively. We have previously¹¹ introduced the generalized PG approximation, denoted GPG $[P]$, where a QM calculation for a particular value of P is approximately corrected using information about the partition function of a reference potential, i.e.,

$$Q^{\text{GPG}[P]} = \frac{Q^{\text{ref}, P=\infty}(T)}{Q^{\text{ref}, P}(T)} Q^{[P]}(T) \quad (11)$$

where $Q^{\text{ref}, P}(T)$ and $Q^{\text{ref}, P=\infty}(T)$ are the partition functions of a reference potential calculated with finite P and infinite P , respectively.

The GPG scheme reduces to the PG scheme if we: (i) set $P = 1$ (which is the classical limit) and (ii) select as our reference potential the harmonic approximation of the true potential at the equilibrium configuration. This choice of reference

potential is especially convenient because an analytical solution for the vibrational partition function of a HO is known⁴ for any value of P provided that the frequencies are real:

$$Q_{\text{vib}}^{\text{HO},P} = \prod_{m=1}^{3n^A-6} q_m^{\text{HO},P}(T) \quad (12)$$

where the 1-D harmonic oscillator partition function for normal mode m with real frequency ω_m is

$$q_m^{\text{HO},P} = \frac{f(\omega_m)^{P/2}}{f(\omega_m)^P - 1} \quad (13)$$

where

$$f = 1 + \frac{R_m^2}{2} + \left(\frac{R_m}{2}\right) \sqrt{4 + R_m^2} \quad (14)$$

and

$$R_m = \frac{\hbar\beta\omega_m}{P} \quad (15)$$

In the $P \rightarrow \infty$ limit, $q_m^{\text{HO},P}$ becomes the exact partition function for a HO

$$q_m^{\text{HO}} = \frac{\exp(-\hbar\beta\omega_m/2)}{1 - \exp(-\hbar\beta\omega_m)} = \frac{1}{2 \sinh(\hbar\beta\omega_m/2)} \quad (16)$$

One limitation of the GPG[P] scheme is that it assumes that a good reference potential can be obtained by considering the local behavior of a system at a single equilibrium configuration. One may further generalize the approximation by allowing the factor that corrects for the use of finite P in the reference potential to be coordinate dependent. We will limit consideration to a harmonic reference potential, but we will allow it to depend on location; thus, the method will be called the local GPG (LGPG) method. The local harmonic reference potential may be chosen as the local Taylor series expansion of the actual potential or as the local Taylor series expansion of a model potential. When we use a $(P+1)$ -point trapezoidal rule quadrature, we label the resulting approximation as LGPG[P], where the label is P rather than $P+1$ because the first and last points are the same. The partition function becomes

$$Q^{\text{LGPG}[P]} = \frac{Q_{\text{fp}}(T)}{\sigma_{\text{sym}}} \times \frac{\int_{\Gamma} d\mathbf{q}_c W^{[P]}(\mathbf{q}_c) \oint D[\mathbf{q}(s)] \delta(\mathbf{q}_c - \bar{\mathbf{q}}) \Phi^{\text{fp}}[\mathbf{q}(s)] \exp\left\{-\frac{\beta}{P} \sum_{i=1}^P V(\mathbf{q}_i)\right\}}{\int_{\Gamma} d\mathbf{q}_c \oint D[\mathbf{q}(s)] \delta(\mathbf{q}_c - \bar{\mathbf{q}}) \Phi^{\text{fp}}[\mathbf{q}(s)]} \quad (17)$$

where, provided the frequencies are all real, the correction factor, $W^{[P]}$, is given by

$$W^{[P]} = \prod_{m=1}^{3n^A-3} \frac{q_m^{\text{HO}}(\omega_m(\mathbf{q}_c), T)}{q_m^{\text{HO},P}(\omega_m(\mathbf{q}_c), T)}; \quad \forall \omega_m^2 \geq 0 \quad (18)$$

The upper limit on the product in eq 18 is $3n^A - 3$ because nonstationary points typically have $3n^A - 3$ modes with nonzero frequencies. At a stationary point three modes will correspond to pure rotations and have zero frequencies; the vibrational partition functions of these modes and any other modes with zero frequencies are set equal to 1. For the special case of $P = 1$ and all real frequencies, the LGPG scheme

reduces to the quantum weighting scheme of Messina, Schenter, and Garrett,³² and we have

$$W^{[P=1]} = \prod_m \frac{\hbar\beta\omega_m(\mathbf{q}_c)/2}{\sinh(\hbar\beta\omega_m(\mathbf{q}_c)/2)}; \quad \forall \omega_m^2 \geq 0. \quad (19)$$

One complication with the LGPG scheme is that we also need an approach to treat modes with imaginary frequencies. Messina et al.³² recommended using a tunneling transmission coefficient derived⁴⁷ for a truncated barrier for the $P = 1$ case, but this is an approximation that has no straightforward generalization to $P > 1$. Instead, when encountering imaginary frequencies, we will adopt

$$W^{[P]} \approx \left(\prod_{m, \omega_m^2 \geq 0} \frac{q_m^{\text{HO}}(\omega_m(\mathbf{q}_c), T)}{q_m^{\text{HO},P}(\omega_m(\mathbf{q}_c), T)} \right) \times \left(\prod_{m, \omega_m^2 < 0} \frac{q_m^{\text{HO},P}(|\omega_m(\mathbf{q}_c)|, T)}{q_m^{\text{HO}}(|\omega_m(\mathbf{q}_c)|, T)} \right) \quad (20)$$

The form of the correction factor for modes with imaginary frequencies is approximate but has the correct qualitative behavior because the use of finite P in the integration of the average energy, V_{ave} , along a particular path causes an increase for a HO with $\omega_m^2 < 0$ of the same amount as the decrease for a HO with $\omega_m^2 > 0$. Provided that the change in βV_{ave} due to the correction for using finite P is small, the correction factor due to an imaginary mode will be approximately the reciprocal of that due to a mode with a real frequency. The correction factor of eq 20 approaches 1 in the $P \rightarrow \infty$ limit. Furthermore, imaginary INM frequencies are usually of low magnitude, so the approximate terms relating to imaginary frequencies will be converged at low values of P . Intermode anharmonicity will also typically converge more rapidly with P . The high frequency motions that are the most difficult to converge in a path integral scheme typically display the least anharmonicity and thus the LGPG[P] corrections may be expected to accurately address the most serious limitation of using finite P values. For these reasons, eq 20 is sufficient for our objective.

2.3. Harmonically Guided Variance Reduction. The difference between the sampling variance of a classical-limit calculation ($P = 1$) and a QM calculation may be thought of as being due to the need to average over all possible paths centered at each value of \mathbf{q}_c in eq 5. The path lengths scale as $\hbar\beta$, so at low temperatures the paths may meander far from the centroid location, and this can lead to a wide variation in their relative contributions to the partition function.

For a harmonic potential with a real frequency, we can analytically calculate the contribution of all paths centered at a given centroid for any given value of P . Furthermore, if we calculate the difference between the contribution of the harmonic representation of the true potential on a specific path and the accurate contribution of that harmonic potential, we can approximate the error due to sampling the true potential for a single path rather than averaging over all possible paths. We will introduce this enhancement by using INM analysis to calculate a local harmonic reference potential V^{ref} and then exclude the quadratic terms that involve imaginary frequencies. This yields what will be called the quadratically stable harmonic reference potential

$$V^{\text{ref,QSH}} = V^{\text{ref}}(\mathbf{q}_c) + \nabla V^{\text{ref}}(\mathbf{q}_c) \cdot (\mathbf{q} - \mathbf{q}_c) + \frac{1}{2} \sum_{m, \omega_m^2(\mathbf{q}_c) > 0} \omega_m^2(\mathbf{q}_c) \eta_m^2 \quad (21)$$

where η_m denotes a mass-scaled INM coordinate with origin \mathbf{q}_c associated with $\omega_m(\mathbf{q}_c)$. The reference potential, V^{ref} , may be taken to be the INM expansion of the true potential if the system is small enough that evaluation of the Hessian is affordable, or it may be some less expensive approximation to the true potential, such as the INM expansion of a model potential.

This leads to a straightforward way to reduce the sampling variance which we denote harmonically guided variance reduction (HGVR). For calculations of $Q^{[P]}$ we modify eq 5 by making the replacement

$$\begin{aligned} & \exp\left\{-\frac{\beta}{P} \sum_{i=1}^P V(\mathbf{q}_i)\right\} \\ & \rightarrow \exp\left\{-\frac{\beta}{P} \sum_{i=1}^P V(\mathbf{q}_i)\right\} + \left[\frac{W_S^{[1]}}{W_S^{[P]}} \exp[-\beta V^{\text{ref}}(\mathbf{q}_c)]\right. \\ & \quad \left. - \exp\left\{-\frac{\beta}{P} \sum_{i=1}^P V^{\text{ref,QSH}}(\mathbf{q}_i)\right\}\right] \end{aligned} \quad (22)$$

where $W_S^{[P]}$ is a modification of $W^{[P]}$ that includes only the factors for stable modes, i.e.,

$$W_S^{[P]} = \left(\prod_{m, \omega_m^2 \geq 0} \frac{q_m^{\text{HO}}(\omega_m(\mathbf{q}_c), T)}{q_m^{\text{HO,P}}(\omega_m(\mathbf{q}_c), T)} \right) \quad (23)$$

For calculations of $Q^{\text{LGPG}[P]}$, we modify eq 17 with the replacement:

$$\begin{aligned} & W^{[P]} \exp\left\{-\frac{\beta}{P} \sum_{i=1}^P V(\mathbf{q}_i)\right\} \\ & \rightarrow W^{[P]} \exp\left\{-\frac{\beta}{P} \sum_{i=1}^P V(\mathbf{q}_i)\right\} + \left[W_S^{[1]} \exp[-\beta V^{\text{ref}}(\mathbf{q}_c)]\right. \\ & \quad \left. - W_S^{[P]} \exp\left\{-\frac{\beta}{P} \sum_{i=1}^P V^{\text{ref,QSH}}(\mathbf{q}_i)\right\}\right] \end{aligned} \quad (24)$$

If we average the last term on the right-hand side of either eqs 22 or 24 over an infinite number of paths having a free-particle distribution, the term will average to zero so the substitution of eqs 22 or 24 does not change the value of converged results. However, when we average over only one or a few paths, the sampling error in the contribution to the partition function from the point \mathbf{q}_c will be significantly reduced.

Note that we only include contributions from INMs with real frequencies because we lack an exact expression for the contributions from modes with imaginary frequencies. However, imaginary frequencies for important regions of configuration space typically are of low magnitude and thus do not contribute greatly to the sampling variance.

The HGVR scheme may be employed with the LGPG $^{[P]}$ scheme or independently. As we will see below, the LGPG $^{[P]}$ results do not converge monotonically with P , although the convergence is monotonic for large P , so if very high accuracy is being targeted, it may be better to extrapolate calculations of $Q^{[P]}$ rather than calculations of $Q^{\text{LGPG}[P]}$.

3. NUMERICAL EXAMPLES

We present numerical examples of the two new methods for H_2O with the Partridge–Schwenke PES⁴⁸ and for H_2O_2 with the PES of Koput, Carter, and Handy.⁴⁹ We have considered both systems previously.^{7,11,41} Because of the low-barrier torsional motion, H_2O_2 is an example of a system for which modes with imaginary INM frequencies are important, and H_2O is an example of a system where imaginary INM frequencies are not expected to contribute significantly.

For both systems we will consider the case where the reference potential is the harmonic expansion of the true potential, and for H_2O_2 , we also consider taking it as the harmonic expansion of a model potential. The model potential consists of the 1-D torsional potential recommended by Koput et al.⁴⁹ added to new 1-D fits of the other degrees of freedom:

$$\begin{aligned} V^{\text{ref}} = & \frac{1}{2} K \{ (\theta_{\text{H}_2\text{O}_2} - \theta_0)^2 + (\theta_{\text{H}_2\text{O}_2} - \theta_0)^2 \} \\ & + D_{\text{OH}} (1 - \exp[-\gamma_{\text{OH}} (R_{\text{H}_2\text{O}_2} - R_0^{\text{OH}})])^2 \\ & + D_{\text{OH}} (1 - \exp[-\gamma_{\text{OH}} (R_{\text{H}_2\text{O}_2} - R_0^{\text{OH}})])^2 \\ & + D_{\text{OO}} \{ (1 - \exp[-\gamma_{\text{OO}} (R_{\text{OO}} - R_0^{\text{OO}})])^2 \} \\ & + \sum_{i=0}^4 c_i \cos(i\phi) \end{aligned} \quad (25)$$

where $K = 138.22$ kcal/rad, $\theta_0 = 1.74376$ rad, $D_{\text{OH}} = 103.47$ kcal/mol, $D_{\text{OO}} = 74.1$ kcal/mol, $R_0^{\text{OH}} = 0.96265$ Å, $R_0^{\text{OO}} = 1.45248$ Å, $\gamma_{\text{OH}} = 2.376$ Å⁻¹, $\gamma_{\text{OO}} = 2.102$ Å⁻¹, $c_0 = 811.3053547$ cm⁻¹, $c_1 = 1037.4$ cm⁻¹, $c_2 = 647.2$ cm⁻¹, $c_3 = 46.9$ cm⁻¹, and $c_4 = 2.7$ cm⁻¹.

For each system we performed calculations using 1×10^9 samples at three temperatures: 296, 600, and 1000 K for H_2O and 300, 600, and 1000 K for H_2O_2 . At 296 and 1000 K for H_2O we adopt as benchmarks the partition functions obtained by Partridge and Schwenke⁴⁸ using sums over Boltzmann factors calculated with accurate eigenvalues; for the other four cases we use well converged ESP extrapolated results as benchmarks. With the large number of samples employed, the statistical sampling errors are small (the largest 1σ sampling error occurs for H_2O at 296 K and is $\sim 0.09\%$, the smallest 1σ sampling error occurs for H_2O at 1000 K and is 0.001%) so the figures displaying partition functions have no need to show error bars. When comparing the relative sampling variances of various methods, we considered a larger number of temperature values and used calculations employing 1×10^6 MC samples. Tabulations of the partition functions plotted, as well as details of numerical parameters employed, are provided in Supporting Information.

None of the finite- P partition functions displayed here were obtained in calculations employing the ESP scheme, although some benchmark $P \rightarrow \infty$ values were obtained by extrapolation of partition functions obtained with this scheme. One reason for this is that, in any one simulation, we would be limited to using P values that are divisors of the largest P used, but we desired a wider range of P values for plotting purposes. A second concern occurs when using the HGVR scheme, because the correction term assumes the centroid of the sampled path is exactly at \mathbf{q}_c . In a set of calculations employing the ESP scheme, we integrate a given path with several different values of P such that P is a divisor of some P^{max} ; e.g., if we select $P^{\text{max}} = 120$, we might also obtain estimations for $P = 60$ and $P = 30$ and

extrapolate to the $P \rightarrow \infty$ limit using these 3 values. For $P < P^{\max}$, our estimator of a path's contribution to the partition function is an average of P^{\max}/P estimators that use different quadratures of the path; these estimators converge monotonically on a path-by-path basis, and each is a valid estimator of a given path's contribution. However, only the quadrature with $P = P^{\max}$ has the centroid of the quadrature points exactly at \mathbf{q}_c , so this is the only choice for which ESP partition functions can be unambiguously labeled $Q^{[P]}$ if this label is to correspond exactly to the result of a Trotter approximation; other values of P will yield partition function estimates that depend slightly on details of the importance sampling. For large values of $P < P^{\max}$, the deviation of the centroid of the quadrature nodes from \mathbf{q}_c is so slight that the resulting partition function estimates are essentially the same as $Q^{[P]}$. Thus, using the HGVR and ESP schemes remains valid, and this is our recommendation for obtaining highly accurate values. However, in the present calculations we are interested in the performance of the LGPG[P] scheme for P values that do not yield qualitatively converged $Q^{[P]}$, and in such situations, the estimators obtained from a calculation using the ESP scheme with $P \ll P^{\max}$ would not correspond exactly to $Q^{[P]}$ and an HGVR correction term would further muddy the meaning of these estimators.

4. RESULTS

Figure 1 compares the results for $Q^{[P]}$ and $Q^{\text{LGPG}[P]}$ as functions of P for H_2O_2 at temperatures of 300, 600, and 1000 K. Figure 2 provides a similar comparison for H_2O at 296 K, 600 K, and 1000 K. In Figure 3 we consider sampling improvements resulting from the HGVR scheme, expressed as the ratio of the variance without and with the scheme, as a function of T for H_2O , where the source for the harmonic reference potential is the true potential and H_2O_2 with two types of sources for the harmonic reference potential, the true potential, and the model potential of eq 25. The data plotted in Figure 3 were obtained with $Q^{[P]}$ for $P = 120$, but the results for $Q^{[P]}$ and $Q^{\text{LGPG}[P]}$ are essentially identical and the variation with P is very slight.

5. DISCUSSION

As seen in Figures 1 and 2, the LGPG[P] scheme converges rapidly with P but in a nonmonotonic manner. This is true both for H_2O_2 , where the torsion leads to imaginary INM frequencies in important regions of configuration space, and for H_2O , where unstable INM modes are not a significant complication.

Figure 1 shows that the LGPG[P] results using the model potential as a source for the harmonic reference potential are of similar quality to those obtained using the true potential. At high temperatures, even $P = 1$ is sufficient to yield good results, whereas at $T = 300$ K, results accurate to within 1.5% are obtained for $P \geq 20$. To obtain a similar accuracy for $Q^{[P]}$ would require a value of $P \approx 130$. Figure 2a shows that LGPG[P] results for H_2O at 296 K are converged to within 0.9% for $P = 20$, whereas this level of accuracy is first achieved in TT calculations with a value for P of about 180, a factor of 9 higher.

Figure 3 shows that the HGVR scheme leads to large variance reductions when the true potential is used as the model potential but more modest reductions when an approximate model potential is used. The best results occur at intermediate T , where the number of samples needed to achieve a desired level of accuracy may be reduced by more

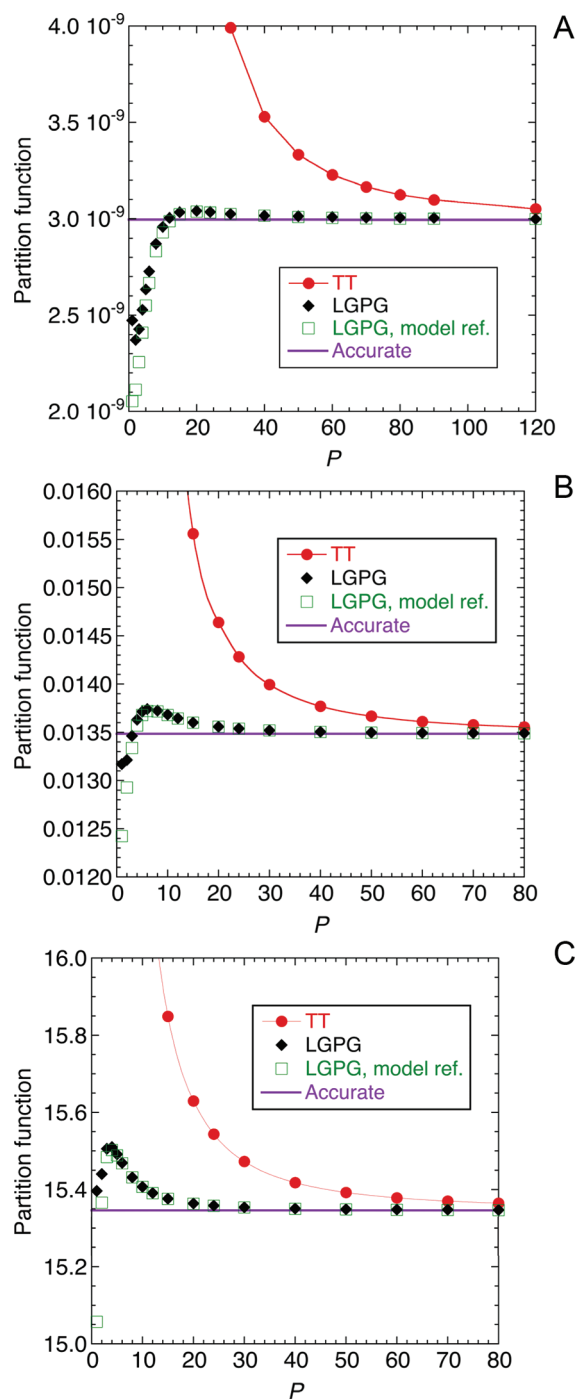


Figure 1. Partition functions for H_2O_2 calculated by the TT approximation compared to LGPG[P] calculations both with the true potential as the source of the harmonic reference potential and with the model potential of eq 25 as the source: (a) 300, (b) 600, (c) 1000 K.

than a factor of 10 by the HGVR technique. In the high- T limit, sampling variances for large- P calculations do not differ dramatically from those for $P = 1$, so the more modest speedups are expected. At low T , anharmonicity becomes increasingly important as the paths explore larger excursions from the centroid location so improvements based on harmonic approximations are more limited.

It is interesting to compare our present calculations for H_2O_2 at 300 K with the result of Chempath et al., who obtained (2.95

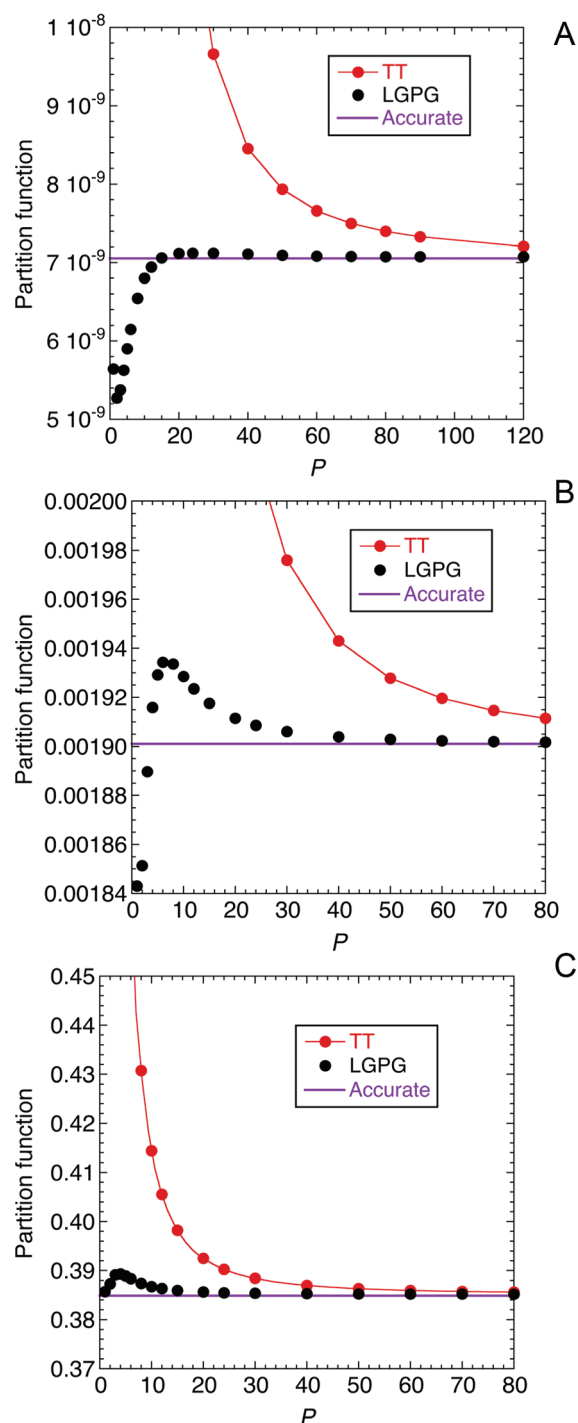


Figure 2. Comparison of partition functions for H_2O calculated by the TT approximation compared to $\text{LGPG}[P]$ calculations: (a) 296, (b) 600, (c) 1000 K.

$\pm 0.03) \times 10^{-9}$ using 10^7 MC samples, and to our prior result of $(2.995 \pm 0.007) \times 10^{-9}$, obtained using 2×10^8 MC samples, where both statistical uncertainties are 1σ . With our current sampling schemes and the HGVR method we observe a 1σ sampling error of about 1% with only 10^6 MC samples, which is about a factor of 10 more efficient than either of these two earlier calculations (the dominant improvement compared to our earlier result comes from the HGVR, but the use of an energy-based stratification scheme, as described in the Appendix Section, is also a significant improvement).

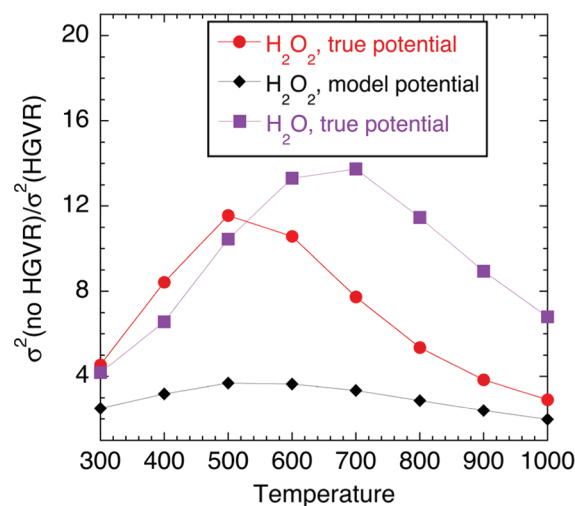


Figure 3. Ratio of the sampling variance without HGVR treatment to the sampling variance with HGVR treatment as a function of T for three test cases.

Chempath et al. also make use of a harmonic reference but restrict its form to have a single minimum so that they may approximate the accurate result for the reference system using analytical results for a harmonic oscillator. This is a significant limitation, and we observe no improvement if we employ the reference potential used by Chempath et al. in our HGVR scheme.

Both the LGPG and HGVR schemes require Hessian calculations of either the true potential or a model potential at every centroid location. For small system sizes the cost of these Hessians is quite affordable (it can be less than the cost for the potential evaluations needed for sampling and numerical quadrature over the path), and the performance gains far outweigh this cost. For large systems Hessian calculations of the true potential would be prohibitively expensive; however, in some circumstances Hessians of a model potential might involve little expense compared to the energy evaluations of the true potential (e.g., if the true potential is obtained by on-the-fly density functional theory calculations and the model potential is obtained by a molecular mechanics potential). In other circumstances, INM calculations based on approximate Hessians may prove to be useful.

6. CONCLUDING REMARKS

We have presented two enhancements to Feynman path integral calculations using information from INM calculations of a harmonic potential. The LGPG scheme significantly improves the convergence with respect to P , the number of path integration points. Using the true potential as the source of the harmonic reference potential leads to the best results, although the cost of Hessian calculations at every configuration may limit this to small system sizes. Using INM calculations of an approximate model potential leads to LGPG calculations that are of similar quality to those of the true potential, but the HGVR scheme is sensitive to the quality of the model potential. The HGVR scheme reduces the sampling variance of MC calculations and thereby improves the efficiency by more than an order of magnitude at intermediate temperatures, and it also delivers significant improvements at low and high T .

■ APPENDIX

In this appendix, we provide additional details of the numerical methods^{8,12,41} used to evaluate the path integrals. The numerical parameters used in the calculations are tabulated in the Supporting Information.

The calculations employed mass-scaled coordinates. For H₂O these are constructed using the mass-scaled vector pointing from one H to the other and the mass-scaled vector pointing from O to the center of mass of H₂. The H₂O₂ coordinates are constructed using the mass-scaled vector pointing from the first H to the first O, the mass-scaled vector pointing from the other O to the other H, and the mass-scaled vector pointing from the center of mass of the second OH to the center of mass of the first OH. For both molecules, these choices of coordinates diagonalize the kinetic energy.⁵⁰ The sampling domain, Γ , is defined by specifying upper and lower boundaries on the magnitudes of each of the unscaled vectors.

Importance sampling is used to select configurations of the centroid configuration. For H₂O, we importance sample the magnitudes of the two Jacobi vectors mentioned above and the angle between these vectors. For H₂O₂, we importance sample the magnitudes of the three vectors mentioned above and the angles between the OH–OH vector and each of the O–H vectors. In each case we use a Gaussian importance sampling function⁴¹ with center parameters taken from the minimum-energy configuration and width parameters that are lightly optimized in small partition function calculations. The sampling uses a zigurat scheme^{41,51} that allows samples to be chosen from the desired distributions (which include Jacobian factors, i.e., the square of the magnitude or the sine of the angle for the coordinates considered here, in addition to the Gaussian sampling functions) with negligible rejection.

In addition to importance sampling, we also employ adaptively optimized stratified sampling⁸ using the value of the potential energy¹² at the centroid position. In the present calculations, we employ 20 strata, the first 19 of which have widths of 0.5 kcal/mol, and we place samples with centroid energies >9.5 kcal/mol in the last stratum. We distribute an initial 10% of the total number of MC samples without regard to the strata. Subsequent MC samples are distributed among the strata to minimize the variance of the calculation with the largest value of P . The optimal distribution is estimated after the initial sampling phase and at 10 additional times as better estimates of the strata variances become available from the sampling already done. The strata volumes are estimated numerically from the distribution of candidate samples generated over the course of the calculation.¹²

We use the sequential sectioning scheme¹² to sample paths according to a free particle distribution. All calculations employ the HGVR scheme. The H₂O calculations use nuclear masses (1836.1527 and 29148.946 m_e) for consistency with the earlier benchmark calculations of Partridge and Schwenke, whereas the H₂O₂ calculations employ atomic masses (1837.1527 and 29156.946 m_e).

■ ASSOCIATED CONTENT

Supporting Information

Tables of parameters used in the numerical calculations and tabulations for all the partition functions plotted in Figures 1 and 2. This material is available free of charge via the Internet at <http://pubs.acs.org>.

■ AUTHOR INFORMATION

Corresponding Author

*E-mail: slmielke@gmail.com; truhlar@umn.edu.

Notes

The authors declare no competing financial interest.

■ ACKNOWLEDGMENTS

This work was supported in part by the National Science Foundation under grant no. CHE09-56776.

■ REFERENCES

- (1) Feynman, R. P.; Hibbs, A. R. *Quantum Mechanics and Path Integrals*; McGraw-Hill: New York, 1965.
- (2) Feynman, R. P. *Statistical Mechanics*; Benjamin: New York, 1972.
- (3) *Monte Carlo Methods in Chemical Physics*; Ferguson, D. M.; Siepmann, J. I.; Truhlar, D. G., Eds.; John Wiley & Sons: New York, 1999.
- (4) Schweizer, K. S.; Stratt, R. M.; Chandler, D.; Wolynes, P. G. *J. Chem. Phys.* **1981**, 75, 1347–1364.
- (5) Mak, C. H.; Andersen, H. C. *J. Chem. Phys.* **1990**, 92, 2953–2965.
- (6) Chao, C. E.; Andersen, H. C. *J. Chem. Phys.* **1997**, 107, 10121–10130.
- (7) Mielke, S. L.; Srinivasan, J.; Truhlar, D. G. *J. Chem. Phys.* **2000**, 112, 8758–8764.
- (8) Srinivasan, J.; Volobuev, Y. L.; Mielke, S. L.; Truhlar, D. G. *Comput. Phys. Commun.* **2000**, 128, 446–464.
- (9) Mielke, S. L.; Truhlar, D. G. *J. Chem. Phys.* **2001**, 114, 621–630.
- (10) Mielke, S. L.; Truhlar, D. G. *Chem. Phys. Lett.* **2003**, 378, 317–322.
- (11) Lynch, V. A.; Mielke, S. L.; Truhlar, D. G. *J. Phys. Chem. A* **2005**, 109, 10092–10099.
- (12) Mielke, S. L.; Truhlar, D. G. *J. Phys. Chem. A* **2009**, 113, 4817–4827.
- (13) Predescu, C.; Doll, J. D. *J. Chem. Phys.* **2002**, 117, 7448–7463.
- (14) Predescu, C.; Doll, J. D. *Phys. Rev. E* **2003**, 67, 026124.
- (15) Predescu, C.; Sabo, D.; Doll, J. D. *J. Chem. Phys.* **2003**, 119, 4641–4654.
- (16) Predescu, C. *Phys. Rev. E* **2005**, 71, 045701.
- (17) Predescu, C. *J. Phys. Chem. B* **2005**, 110, 667–670.
- (18) Chempath, S.; Predescu, C.; Bell, A. T. *J. Chem. Phys.* **2006**, 124, 234101–234112.
- (19) Coalson, R. D.; Freeman, D. L.; Doll, J. D. *J. Chem. Phys.* **1986**, 85, 4567–4583.
- (20) Coalson, R. D.; Freeman, D. L.; Doll, J. D. *J. Chem. Phys.* **1989**, 91, 4242–4248.
- (21) Coalson, R. D. *J. Chem. Phys.* **1986**, 85, 926–936.
- (22) Cao, J.; Berne, B. J. *J. Chem. Phys.* **1990**, 92, 7531–7539.
- (23) Messina, M.; Garrett, B. C.; Schenter, G. K. *J. Chem. Phys.* **1994**, 100, 6570–6577.
- (24) Friesner, R. A.; Levy, R. M. *J. Chem. Phys.* **1984**, 80, 4488–4495.
- (25) Zhang, P.; Levy, R. M.; Friesner, R. A. *Chem. Phys. Lett.* **1988**, 144, 236–242.
- (26) Jang, S.; Jang, S.; Voth, G. A. *J. Chem. Phys.* **2001**, 115, 7832–7842.
- (27) Takahashi, M.; Imada, M. *J. Phys. Soc. Jpn.* **1984**, 53, 3765–3769.
- (28) Hwang, J.-K.; Warshel, A. *J. Phys. Chem.* **1993**, 97, 10053–10058.
- (29) Hwang, J.-K. *Theor. Chem. Acc.* **1999**, 101, 359–363.
- (30) Ceperley, D. *Rev. Mod. Phys.* **1995**, 67, 279–355.
- (31) Feynman, R. P.; Kleinert, H. *Phys. Rev. A* **1986**, 34, S080–S084.
- (32) Messina, M.; Schenter, G. K.; Garrett, B. C. *J. Chem. Phys.* **1993**, 98, 4120–4127.
- (33) Mielke, S. L.; Truhlar, D. G. *J. Chem. Phys.* **2001**, 115, 652–662.
- (34) Voth, G. A. *J. Chem. Phys.* **1991**, 94, 4095–4096.
- (35) Voth, G. A. *Phys. Rev. A* **1991**, 44, S302–S305.
- (36) Giachetti, R.; Tognetti, V. *Phys. Rev. Lett.* **1985**, 55, 912–915.

- (37) Giachetti, R.; Tognetti, V. *Phys. Rev. B* **1986**, 33, 7647–7658.
- (38) Giachetti, R.; Tognetti, V. *J. Magn. Magn. Mater.* **1986**, 54–57 (Part 2), 861–862.
- (39) Cuccoli, A.; Giachetti, R.; Tognetti, V.; Vaia, R.; Verrucchi, P. *J. Phys.: Condens. Matter* **1995**, 7, 7891–7938.
- (40) Wong, K.-Y.; Gao, J. *J. Chem. Theory Comput.* **2008**, 4, 1409–1422.
- (41) Lynch, V. A.; Mielke, S. L.; Truhlar, D. G. *J. Chem. Phys.* **2004**, 121, 5148–5162.
- (42) De Raedt, H.; De Raedt, B. *Phys. Rev. A* **1983**, 28, 3575–3580.
- (43) Janke, W.; Sauer, T. *Phys. Lett. A* **1992**, 165, 199–205.
- (44) Suzuka, M. *Phys. Lett. A* **1993**, 180, 232–234.
- (45) Makri, N.; Miller, W. H. *J. Chem. Phys.* **1989**, 90, 904–911.
- (46) Pitzer, K. S.; Gwinn, W. D. *J. Chem. Phys.* **1942**, 10, 428–440.
- (47) Skodje, R. T.; Truhlar, D. G. *J. Phys. Chem.* **1981**, 85, 624–628.
- (48) Partridge, H.; Schwenke, D. W. *J. Chem. Phys.* **1997**, 106, 4618–4639.
- (49) Koput, J.; Carter, S.; Handy, N. C. *J. Phys. Chem. A* **1998**, 102, 6325–6330.
- (50) Hirschfelder, J. O.; Dahler, J. S. *J. Chem. Phys.* **1956**, 24, 1258–1258.
- (51) Marsaglia, G.; Tsang, W. W. *J. Stat. Software* **2000**, 5, 1–7.